Spatiotemporal Variability in Land Surface Temperature Over the Mountainous Region Affected by the 2008 Wenchuan Earthquake From 2000 to 2017

Zhao Wei

Institute of Mountain Hazards and Environment,

Chinese Academy of Sciences

2019-09-09

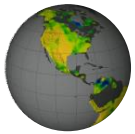

Wenchuan Earthquake

Summary of earthquake-triggered landslide inventories.

No.	Country	Region	Date	M_w	M_s	Type	Number	Area (km^2)	References
1	China	Lushan	2013/4/20	6.6	7.0	Point	3878		Xu, 2013b
						Point	15,639		Xu and Xu, 2014a
2	Spain	Lorca	2011/5/11	5.1		Point	>250		Alfaro et al., 2012
3	China	Yushu	2010/4/14	6.9	7.1	Polygon	2036	1.194	Xu et al., 2013b; Xu and Xu, 2014b
						Point	282		Yin et al., 2010
4	Haiti	Port-au-prince	2010/1/12	7.0		Polygon	30,828	15.736	Xu and Xu, 2012b; Xu et al., 2012c, 2014a
						Point	>7000		Harp et al., 2011b
						Polygon	4490	8	Gorum et al., 2013
5	Japan	Iwate–Miyagi	2008/6/14	6.9	7.2	Point	4161	10.2	Yagi et al., 2009
6	China	Wenchuan County	2008/5/12	7.9	8.0	Polygon, Top point, Centroid	197,481	1160	Xu and Xu, 2012a; Xu et al., 2014c
						Polygon	56,000	811	Dai et al., 2011
						Polygon	48,007	711.8	Xu et al., 2009a, b
						Polygon	73,367	565.8	Parker et al., 2011
						Point	60,000		Gorum et al., 2011
						Point	<10,000		Qi et al., 2010
						Point	16,704		Huang and Li, 2009a
						Point	<10,000		Huang and Li, 2009b
7	Chile	Aysén Fjord	2007/1/22	6.2	6.3	Polygon	538	17	Sepúlveda et al., 2010
8	India–Pakistan	Kashmir	2005/10/8	7.6	7.7	Polygon	1293		Owen et al., 2008
						Point	2424		Sato et al., 2007
						Polygon	2252	61	Kamp et al., 2008
9	Japan	Niigata	2004/10/23	6.6	6.8	Polygon	1212	7.99	Wang et al., 2007
						Polygon	>1000		Chigira and Yagi, 2006
						Polygon	362		Sassa, 2005
						Polygon	1353		Sato et al., 2005
						Polygon	4438		Sekiguchi and Sato, 2006
10	China	Taiwan	1999/9/21	7.6	7.3	Polygon	~10,000		Liao and Lee, 2000; Wang et al., 2003; Khazai and Sitar, 2004
						Polygon	~20,000		Wang et al., 2002
11	Italy	Umbria–Marche	1997/9/26	6	5.9	Polygon	200		Marzorati et al., 2002
12	Japan	Hyogo-ken Nanbu	1995/1/17	6.9	6.8	Point	674		Fukuoka et al., 1997
13	America	Northridge, California	1994/1/17	6.7	6.8	Polygon	>11,000	23.8	Jibson and Harp, 1994; Harp and Jibson, 1996
14	America	Loma Prieta, California	1989/10/17	6.9	7.1	Point	>1046		Keefer, 2000
15	Ecuador		1987/3/5	7	6.9	Point			Tibaldi et al., 1995; Schuster et al., 1996
16	America	Coalinga	1983/5/2	6.2	6.7	Polygon			Harp et al., 2011a
17	Italy	Irpinia	1980/11/23	6.9	6.9	Polygon			Harp and Keefer, 1989; Wasowski et al., 2002
18	America	Mammoth Lakes, California	1980/05/25–27		6.1	Polygon	5200	6	Harp et al., 1984, 2011a
19	Italy	Friuli	1976/5/6		6.4	Point			Govi, 1977; Harp et al., 2011a
20	Guatemalan		1976/2/4		7.5	Polygon	50,000		Harp et al., 1978, 1981, 2011a
21	America	San Fernando, California	1971/2/9		6.5	Polygon	>1000		Morton, 1971; Harp et al., 2011a
22	Peru		1970/5/31	7.8	7.9	Point	>1000		Plafker et al., 1971; Harp et al., 2011a
23	Japan	Imaichi	1949/12/26		6.4	Point			Morimoto, 1951; Harp et al., 2011a
24	New Zealand	Murchison	1929/6/17	7.7	7.8	Point	>7400	200	Adams, 1980; Pearce and O'Loughlin, 1985; Pearce and Watson, 1986
25	America	New Madrid	1811/12/16	8.3	8.8	Point	>220		Jibson and Keefer, 1989

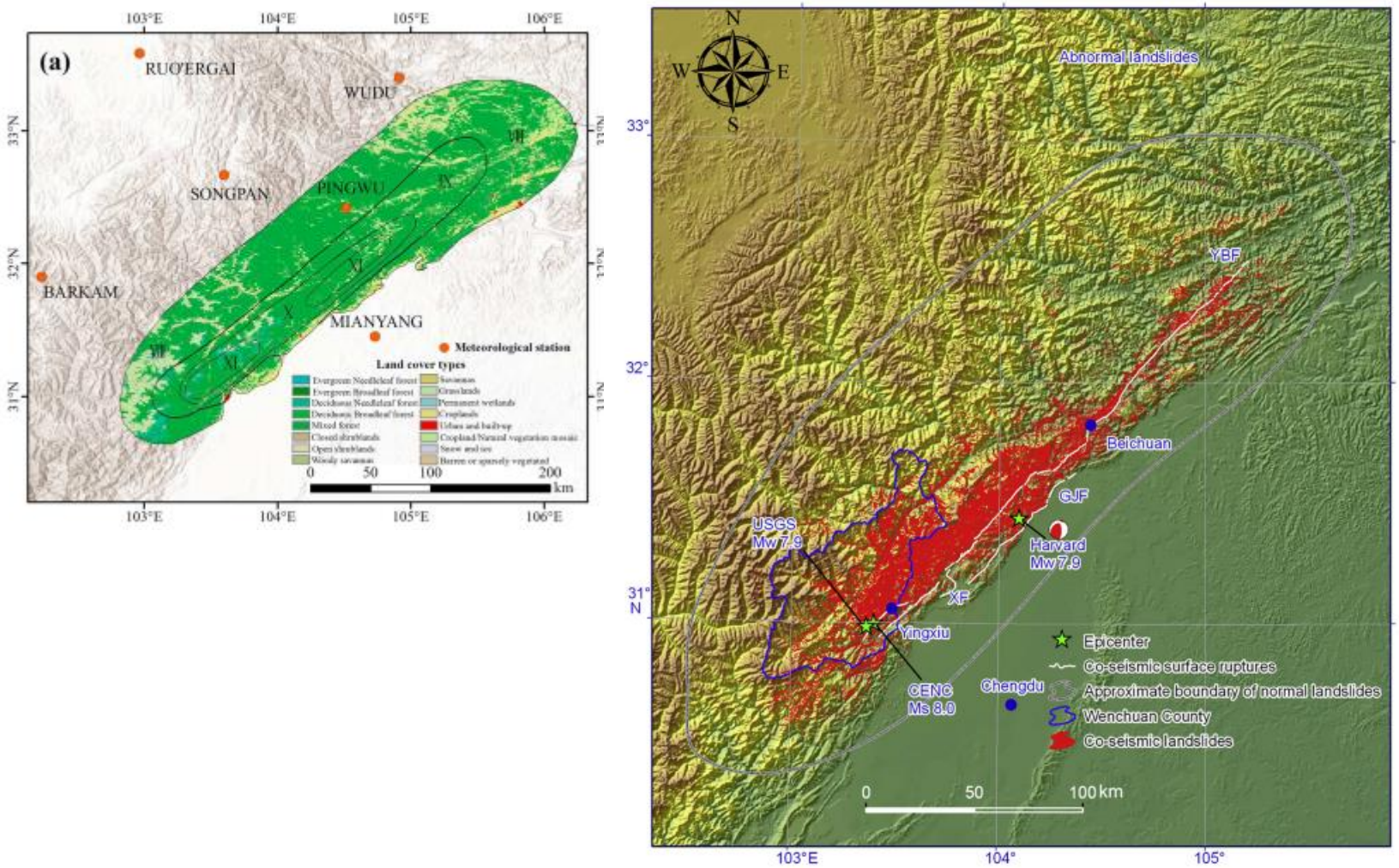

Spatial distribution of landslides triggered by the 2008 Wenchuan earthquake, China and remote images used for landslide visual interpretation pre- and post-earthquake.YBF is the Yingxiu-Beichuan fault; GJF is the Guanxian-Jiangyou fault; XF is the Xiaoyudong fault. USGS is U.S. Geological Survey; CENC is China Earthquake Network Center; Havard is Havard University.

C. Xu / Geoscience Frontiers 6 (2015) 825-836

The postearthquake geohazard investigation conducted by Yin et al. (2009) showed that the earthquake directly caused more than15,000 geohazards in the forms of landslides, rockfalls, and debris flows.

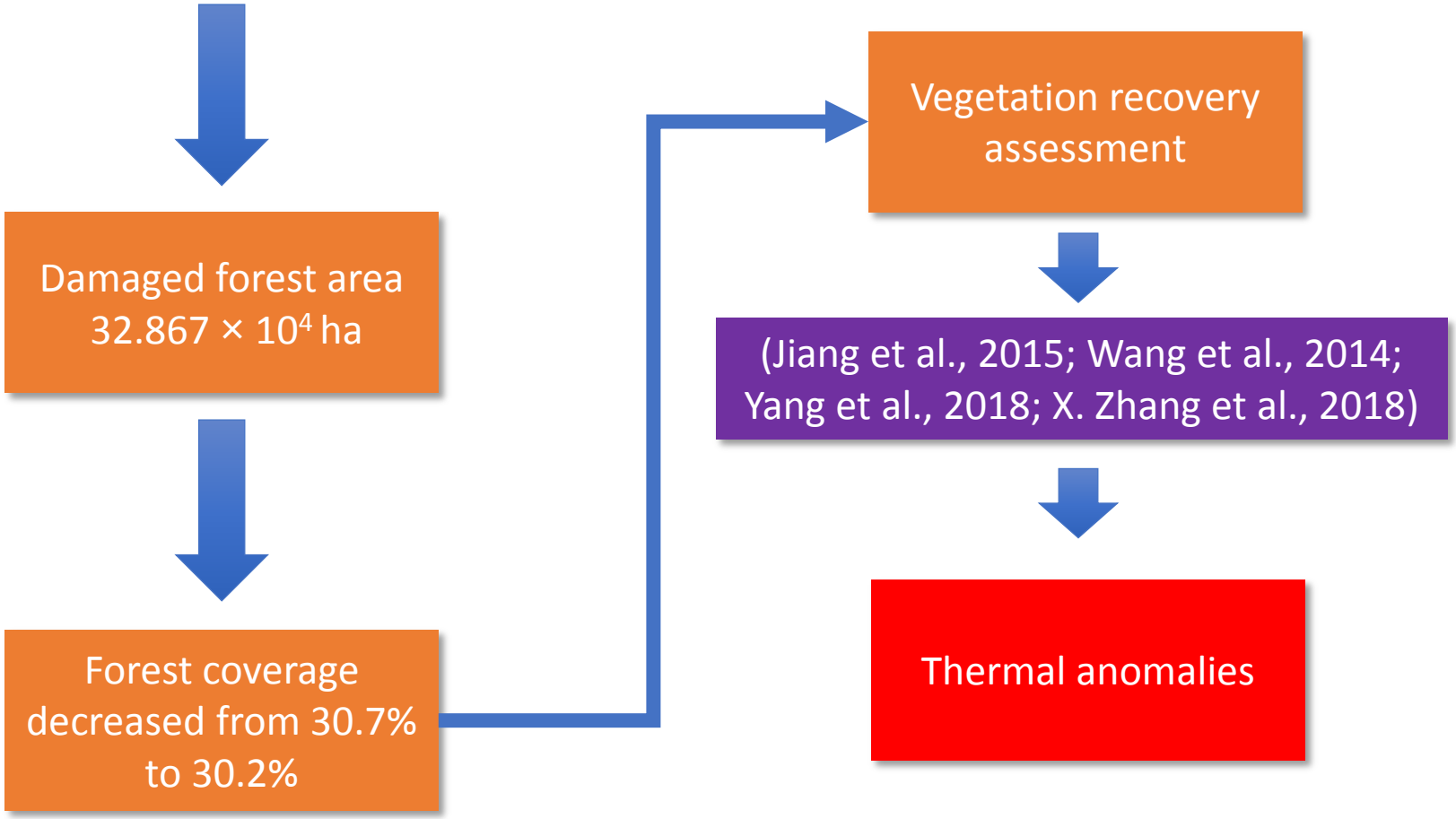

the forestry department of the Sichuan Province

Data:

MODIS Land Surface Temperature and Emissivity (MOD11)

Overview

The Land Surface Temperature
1km pixels by the generalized
day/night algorithm. In the sp
32 are estimated from land co
lower boundary air surface ter
for optimal retrieval. In the da
surface emissivities are retriev
in seven TIR bands. The produ
observation time, view angles,

MODIS Vegetation Index Products (NDVI and EVI)

Overview

MODIS vegetation indices, produced on 16-day intervals and at multiple spatial resolutions, provide consistent spatial and temporal comparisons of vegetation canopy greenness, a composite property of leaf area, chlorophyll and canopy structure. Two vegetation indices are derived from atmospherically-corrected reflectance in the red, near-infrared, and blue wavebands; the normalized difference vegetation index (NDVI), which provides continuity with NOAA's AVHRR NDVI time series record for historical and climate applications, and the enhanced vegetation index (EVI), which minimizes canopy-soil variations and improves sensitivity over dense vegetation conditions. The two products more effectively characterize the global range of vegetation states and processes.

Methods:

$$f(d) = \mathrm{MAST} + \mathrm{YAST} \cdot \sin\left(\frac{2\pi(d+\theta)}{365}\right)$$

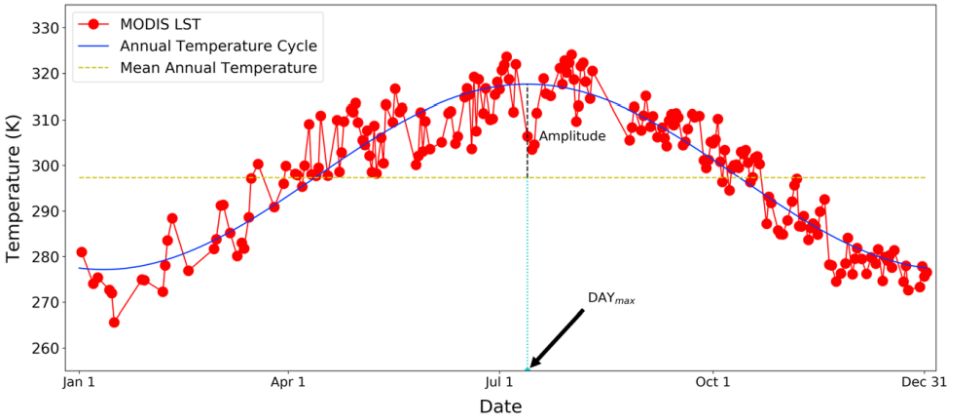

where d is the day of the cycle. The other three parameters are typically referred to as ACPs, including mean annual surface temperature (MAST), yearly amplitude of surface temperature (YAST), and phase shift (θ).

$$\begin{cases} T_{\max,\mathrm{D}} = \mathrm{MAST_D} + \mathrm{YAST_D} \\ T_{\min,\mathrm{D}} = \mathrm{MAST_D} - \mathrm{YAST_D} \\ T_{\max,\mathrm{N}} = \mathrm{MAST_N} + \mathrm{YAST_N} \\ T_{\min,\mathrm{N}} = \mathrm{MAST_N} - \mathrm{YAST_N} \end{cases}$$

The average annual cycle parameter values during the period from 2000 to 2017. (a) Daytime mean annual surface temperature (MAST) in kelvins, (b) daytime yearly amplitude of surface temperature (YAST) in kelvins, (c) the day of maximum temperature at the daytime, (d) nighttime MAST in kelvins, (e) nighttime YAST in kelvins, and (f) the day of maximum temperature at the nighttime.

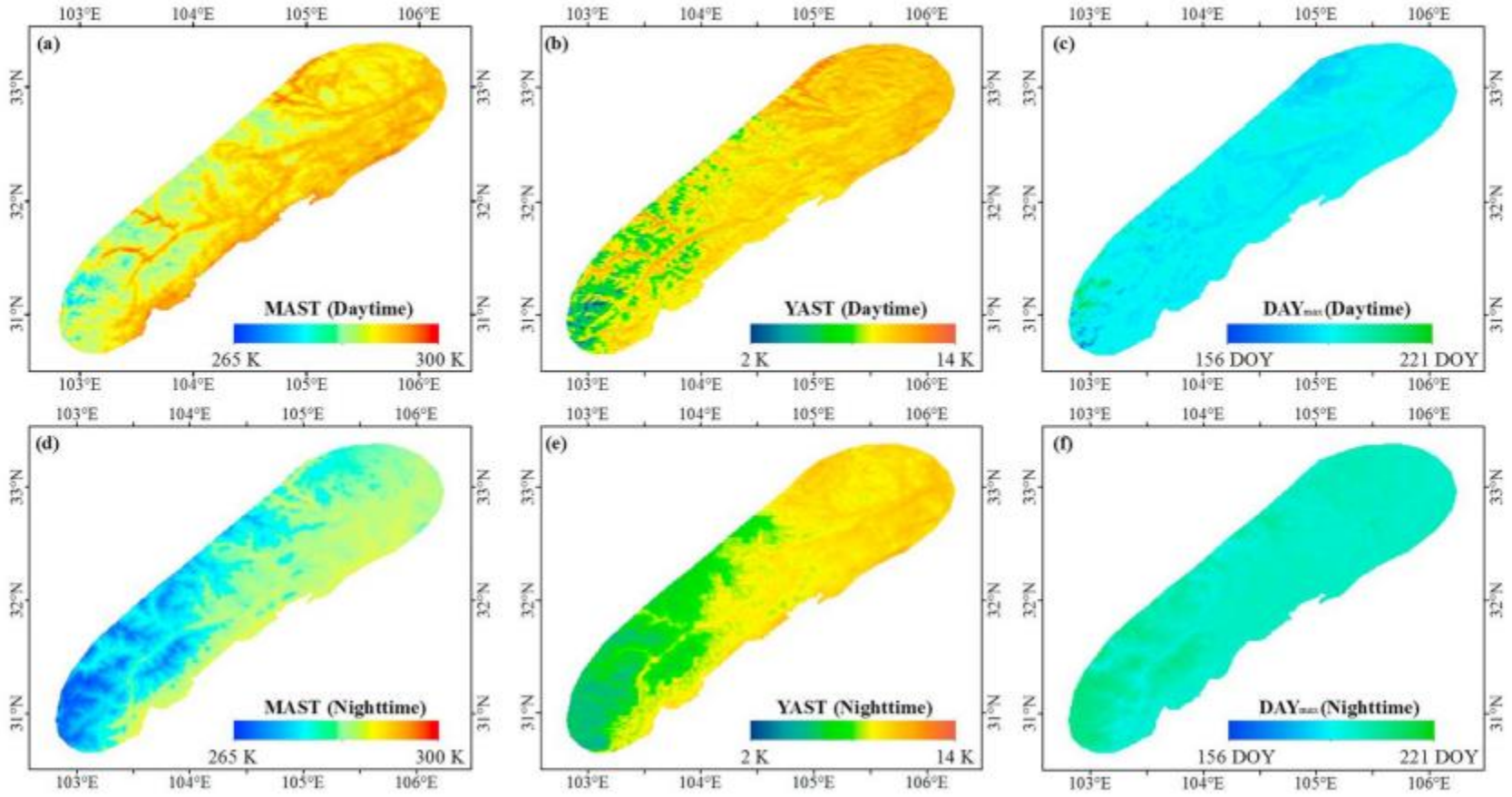

(a – c) The daytime annual cycle parameter change rates with a signi fi cant trend from 2000 to 2017. MAST = mean annual surface temperature; YAST = yearly amplitude of surface temperature.

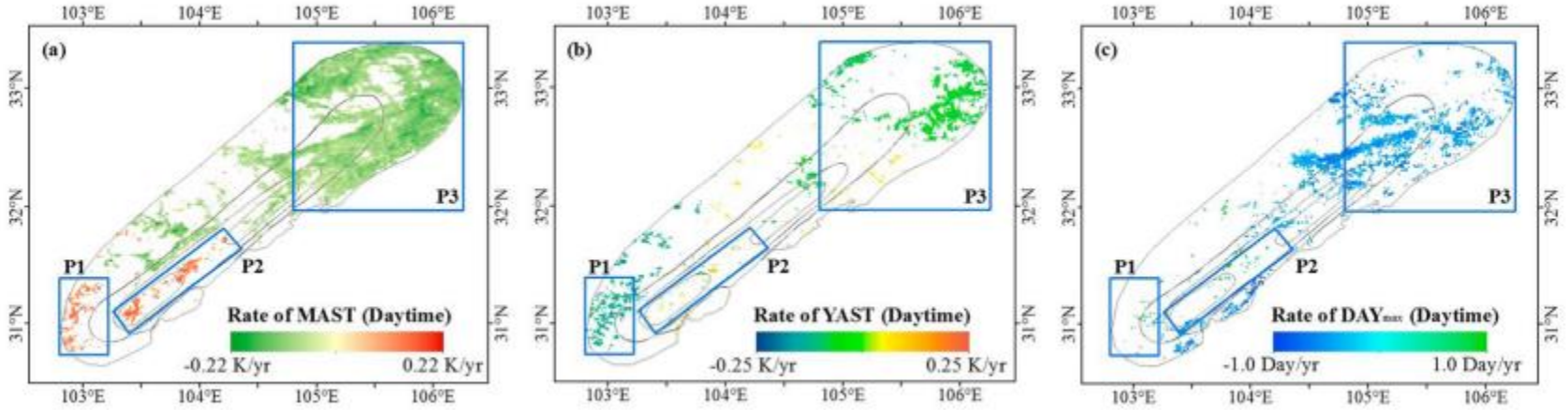

(a – c) The nighttime annual cycle parameter change rates with a signi fi cant trend from 2000 to 2017. MAST = mean annual surface temperature; YAST = yearly amplitude of surface temperature.

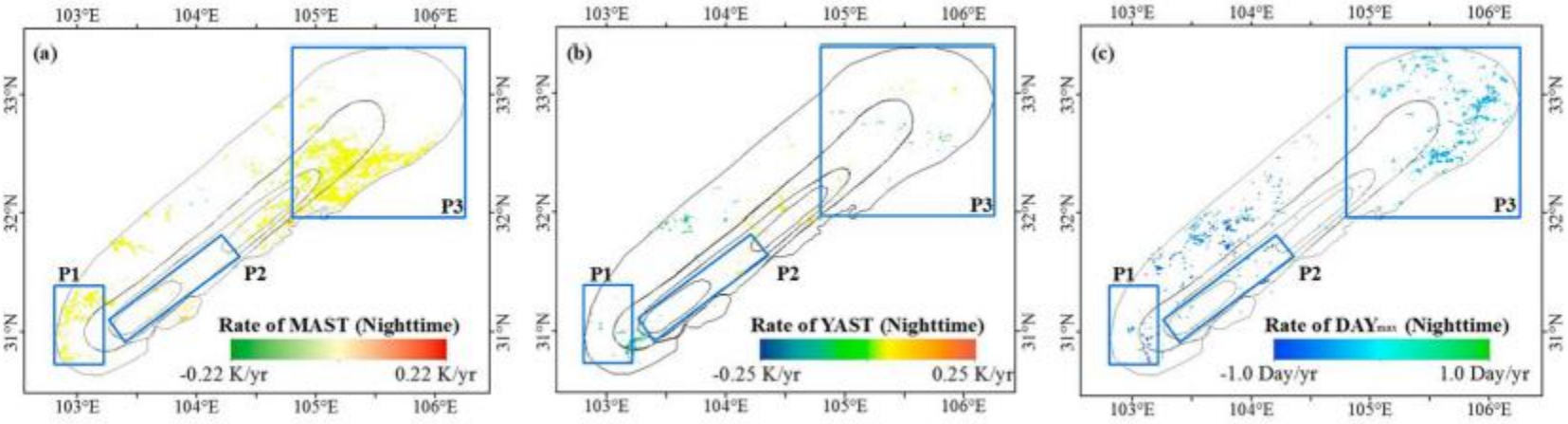

Change Mechanisms

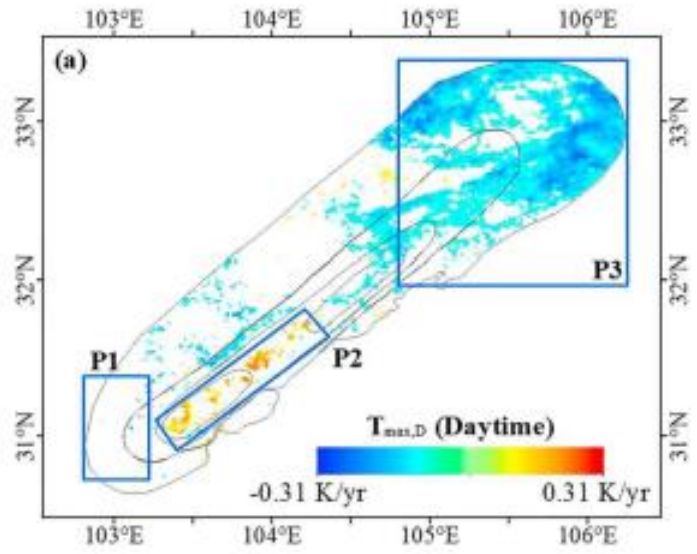

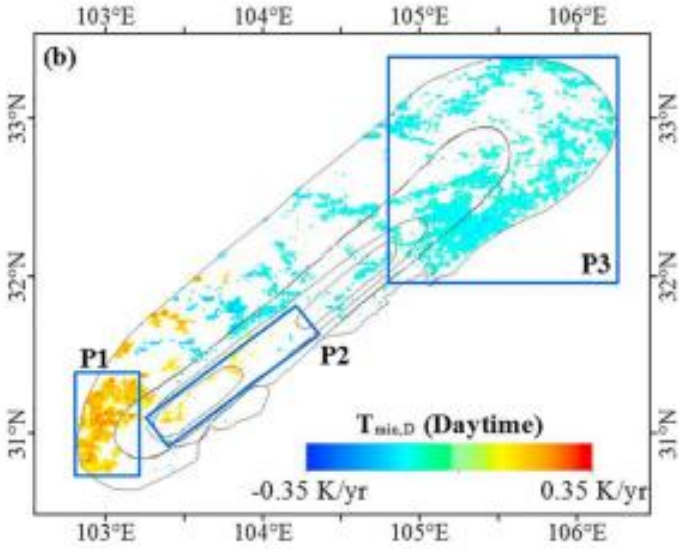

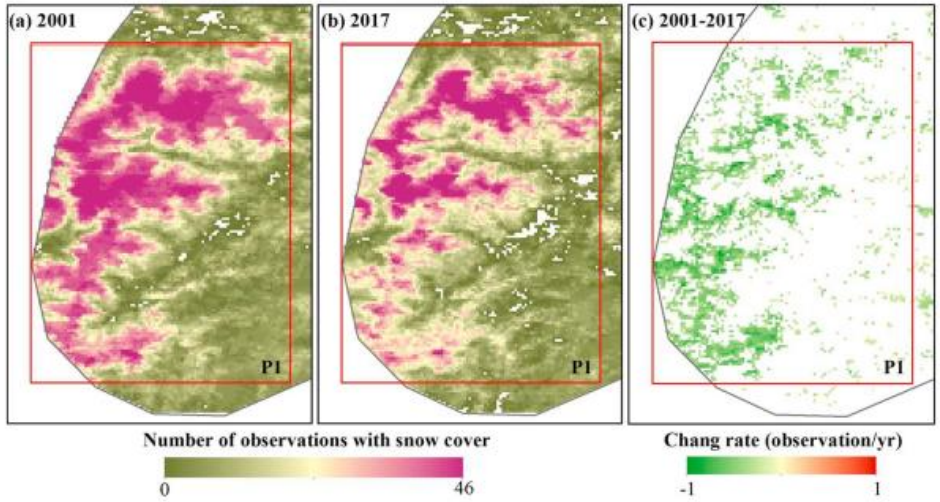

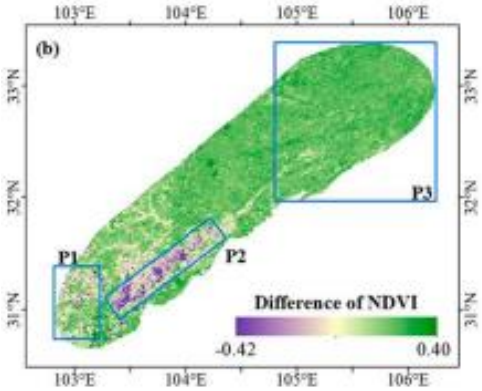

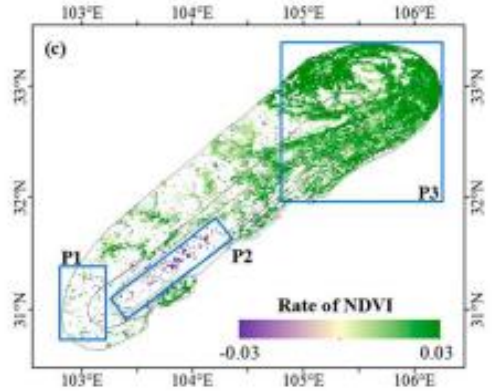

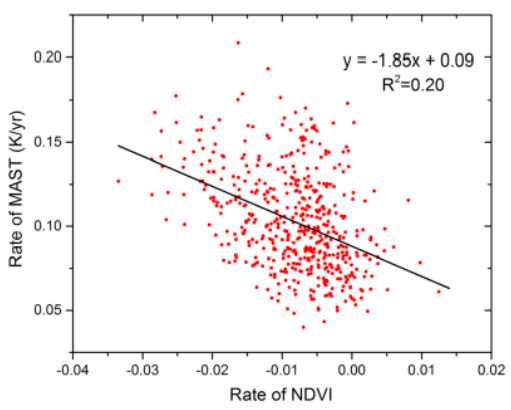

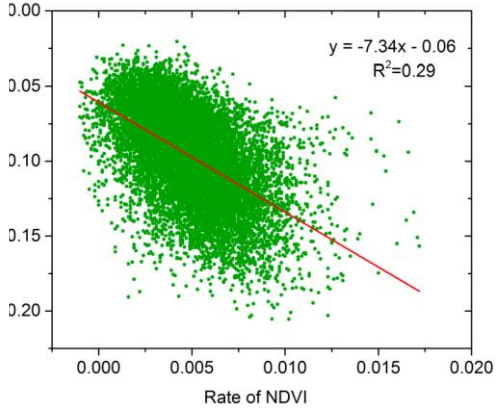

Climate Change Background

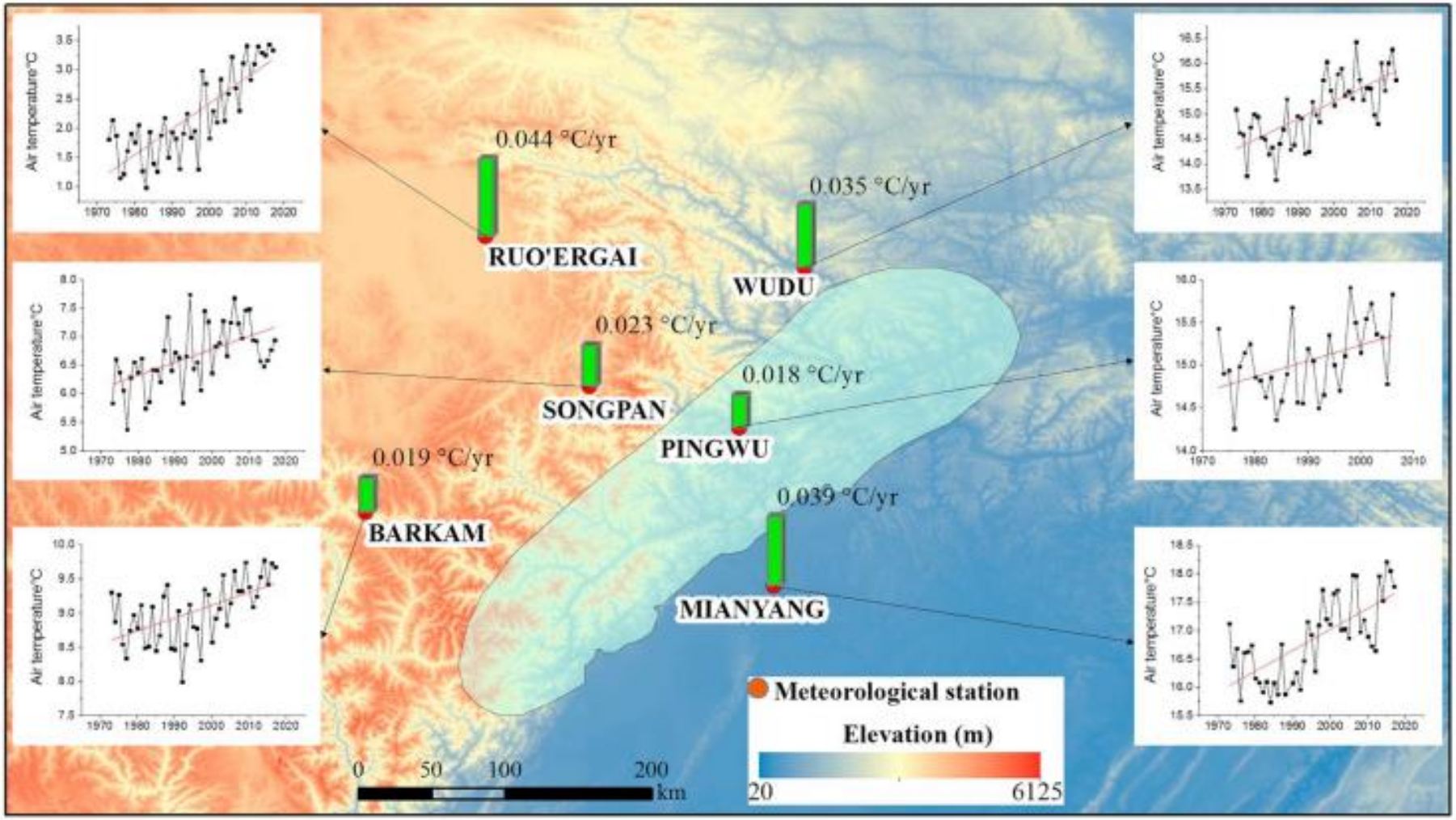

A significant warming environment

Implications From the Changes

- The increase in surface temperature will inhibit vegetation recovery due to a reduction in soil water conservation ability and a decrease in soil moisture availability.

- Barren surface exposure with abundant loose debris enables the occurrence of debris fl ows and landslides under heavy rainfall.

- Vegetation coverage improvement regulates the global warming effect in the mountainous region. A positive feedback effect for the local ecoenvironment can be detected according to the increase in NDVI.

- the high sensitivity of the high mountain area to climate change, especially for snow covered surfaces. Potentially, snow melt water supplementation will be threatened.

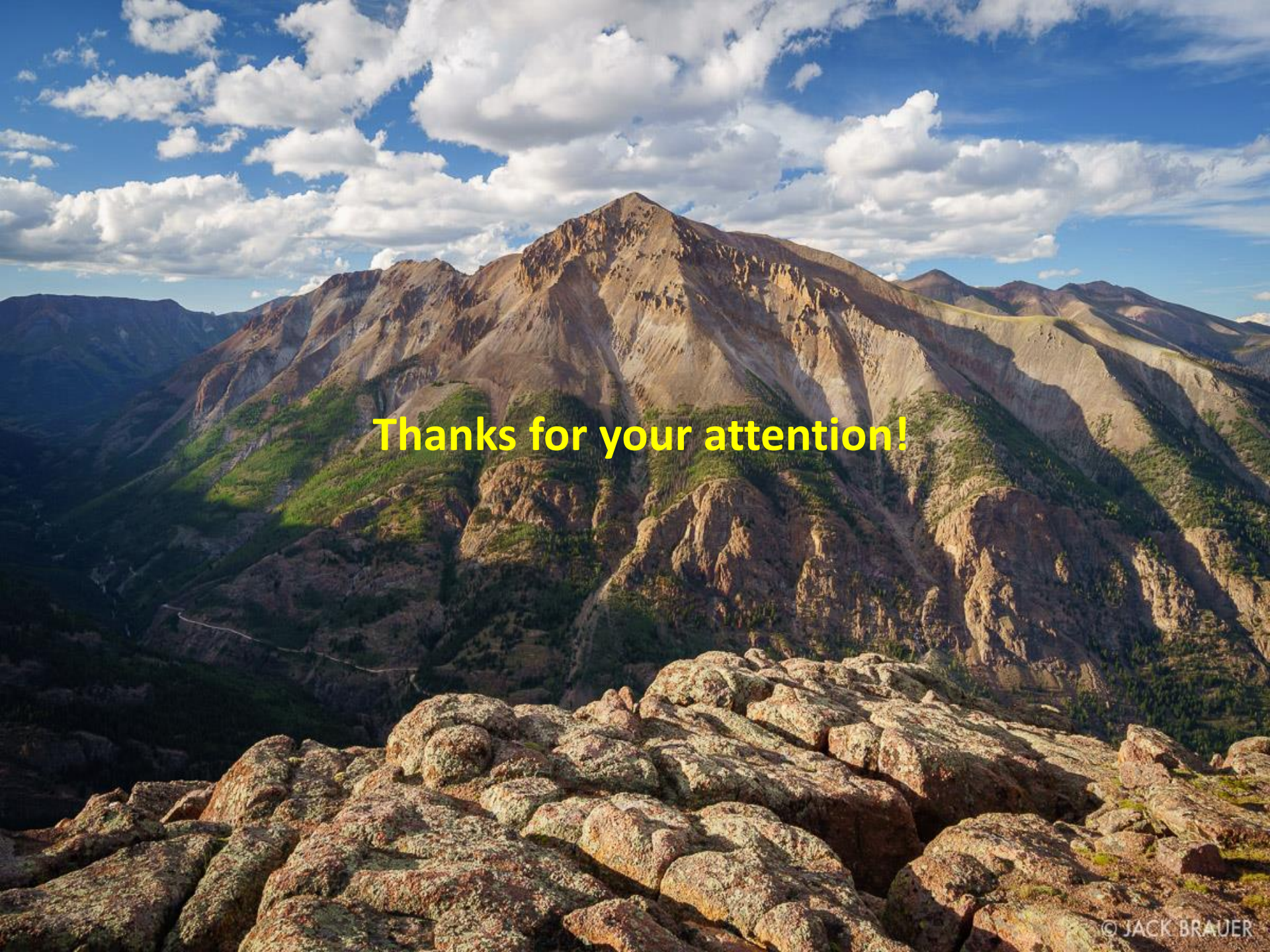
Thanks for your attention!
© JACK BRAUER